Electronic Supplementary Material (ESI) for EES Catalysis.

Supporting Information

Cyclic Voltammetry Activation of Magnetron Sputtered Copper-Zinc Bilayer Catalysts for Electrochemical CO_2 Reduction

Yang Fu, Shilei Wei, Dongfeng Du, Jingshan Luo*

Institute of Photoelectronic Thin Film Devices and Technology, Key Laboratory of Photoelectronic Thin Film Devices and Technology of Tianjin, Ministry of Education Engineering Research Center of Thin Film Photoelectronic Technology, Frontiers Science Center for New Organic Matter, Nankai University, Tianjin 300350, China.

*E-mail: jingshan.luo@nankai.edu.cn

Experimental details.

Chemical and electrolyte. GDL (26-BC) was purchased from Sigrate. The metal targets (Zn and Cu) were bought from Zhongcheng New Material Technology Co., Ltd. KOH (99.99%, metals basis), $KHCO_3$ (≥99.99%, metals basis) were bought from Aladdin. CO_2 (99.999%) gases were purchased from Air Liquid Co., Ltd.

Preparation of the electrodes.

Preparation of Cu-GDE catalyst: As shown in **Scheme 1**, we sputtered a layer of metallic copper on the gas diffusion electrode by magnetron sputtering. The metal Cu target with a purity of 99.999% was sputtered onto the GDL by DC magnetron sputtering at the pressure of 0.5 Pa in the Ar atmosphere, with an argon flow of 80 sccm. Moreover, the sputtering power was adjusted to 100 W for 10 min. Then, the copper sputtered on GDL was placed in a vacuum drying oven for future use.

Preparation of Cu-Zn layered bimetallic catalyst on the GDL: Subsequently, the metal copper target in the previous step was taken out and replaced with a metal Zn target (99.999%). Copper on GDL was used as the substrate and the pressure was set at 0.5 Pa with the Ar gas flow rate of 80 sccm. The sputtering power was set to 45 W for 5 min to obtain a layered Cu-Zn bimetallic catalyst. Then, the as-obtained Cu-Zn bimetallic catalyst was put into a vacuum drying oven to dry and stored for future use.

Preparation of Cu-Zn-CV-GDE catalyst: The layered Cu-Zn bimetallic catalyst on the gas diffusion layer electrode was cut into a size of 2.5 cm×2 cm and used as a working electrode. It should be noted the size of the catalyst was immersed in the solution with the size of 2 cm × 2 cm. The working electrode was performed cyclic voltammetry treatment by using a three-electrode system. The metal platinum mesh with a size of 2 cm × 2 cm was used as the counter electrode. Ag/AgCl saturated with KCl aqueous solution was used as a reference electrode, and the electrolyte was 0.1 M $KHCO_3$ solution. In addition, the voltage range of cyclic voltammetry was from -0.4 V to 2.6 V vs. RHE at the scan rate of 100 mV s^{-1} for 15 cycles. After the electrochemical CV treatment, the samples were taken out and washed with deionized water. Then it was dried under N_2 atmosphere and stored in a vacuum oven for future use.

Preparation of Zn-GDE catalyst: We used magnetron sputtering to sputter a layer of metal Zn on gas diffusion electrode. Specifically, the metal Zn target with a purity of 99.999% was sputtered onto the gas diffusion electrode by DC magnetron sputtering under the pressure of 0.5 Pa and the Ar flow rate was 80 sccm. The sputtering power was adjusted to 45 W for 12 min. After the sputtering was completed, Zn prepared by sputtering on the gas diffusion electrode was placed in a vacuum drying oven for storage for future use.

Electrochemical measurements

Flow cell test. The electrocatalytic CO_2 reduction performance of the three catalysts on GDE was tested by using flow cell. IrO_2 and Ag/AgCl electrodes were used as anode and reference electrodes, respectively. Moreover, the exposed size of the working electrode was 1 cm^2 (1 cm ×1 cm). 1.0 M KOH solution was used as both catholyte and anolyte. Notably, when calculating the FE of gas product, the outlet flow rate was needed by using the soap bubble method. During this test, the inlet CO_2 gas flow rate was 10 sccm and the outlet flow rate was 6~8 sccm. In addition, the inlet gas flow rate was controlled by a mass flow controller.

Electrocatalytic CO_2 reduction product analysis. During the CO_2 reduction test, electrolysis was at a constant current for a certain period, and the reaction cell was connected to the GC. The gas product can be detected and analyzed by gas chromatography (GC, Fuli 9790 Plus Instruments). The gas chromatograph collected the gas products every 9 minutes. TCD was used to analyze and detect hydrogen, and two FIDs were responsible for analyzing and detecting gases, such as methane, carbon monoxide, ethylene and ethane. For liquid products, the quantification was carried out in high-performance liquid chromatography (HPLC, Agilent 1260). The carrier liquid was 5 mM H_2SO_4 solution, and the collected catholyte (900 μL) was acidified with 100 μL of 4.5 M H_2SO_4 for future use. The FE of the corresponding liquid products was calculated by dividing the charge of each gas or liquid products by the total charge at the given time.

Material characterizations. The scanning electron microscopy (SEM) images were obtained by Field-emission scanning electron microscopy (Apreo, S LoVac). Transmission electron microscopy (TEM) images, including High-resolution transmission electron microscopy (HRTEM), were acquired by an FEI Talos F200X G2. The X-ray diffraction (XRD) measurements were carried out on Rigaku using (2θ) mode with a Cu Kα radiation source (λ = 1.5406 Å). X-ray photoelectron spectroscopy (XPS) instruments were measured by Thermo Scientific ESCALAB 250X using Al Kα radiation.

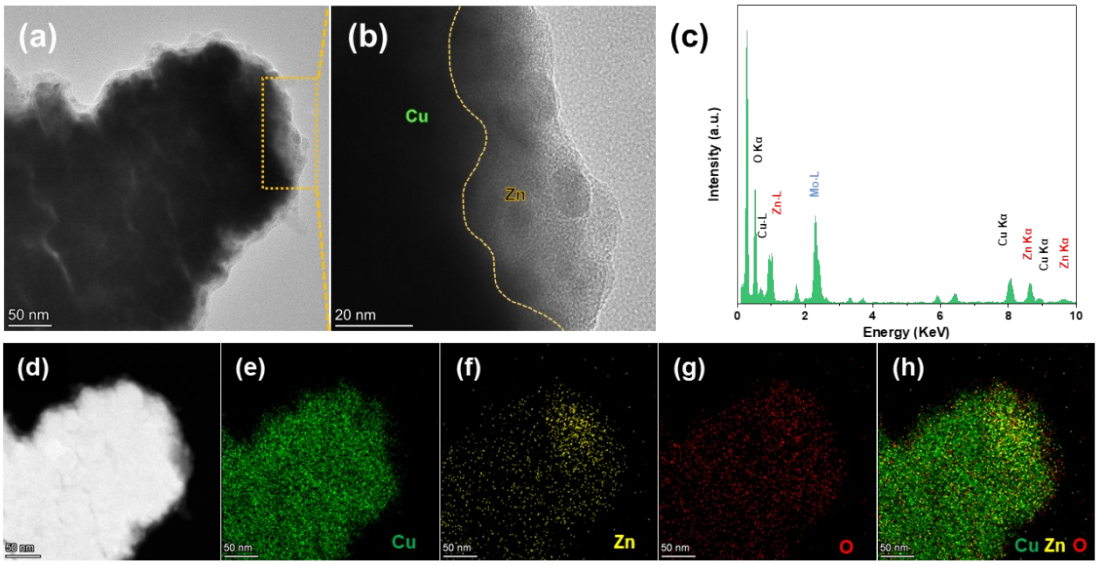

Figure S1. (a) TEM and (b) HRTEM and (c) EDS analysis of representative Cu-Zn-GDE catalysts. (d) High Angle annular dark field transmission (HADDF-STEM) diagram related to the catalyst, TEM EDS-mapping diagram of the catalyst, mapping superposition diagram of corresponding (e) Cu, (f) Zn, (g) O, and (h) Cu, Zn, O elements.

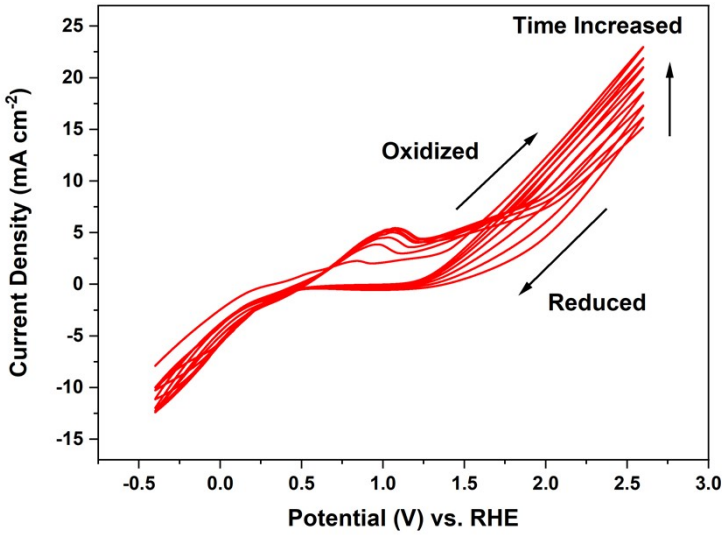

Figure S2. Cyclic voltammetry curves of Cu-Zn-GDE catalyst were tested in 0.1 M $KHCO_3$ aqueous solution and the potential range was -0.4 V~-2.6 V vs. RHE.

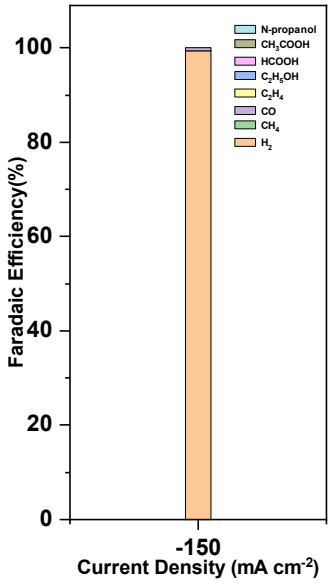

Figure S3. Faradaic Efficiency of various products of Cu-Zn-CV GDE catalyst at the current densities of -150 mA cm^{-2} during the electrocatalytic reduction under N_2 atmosphere in the flow cell.

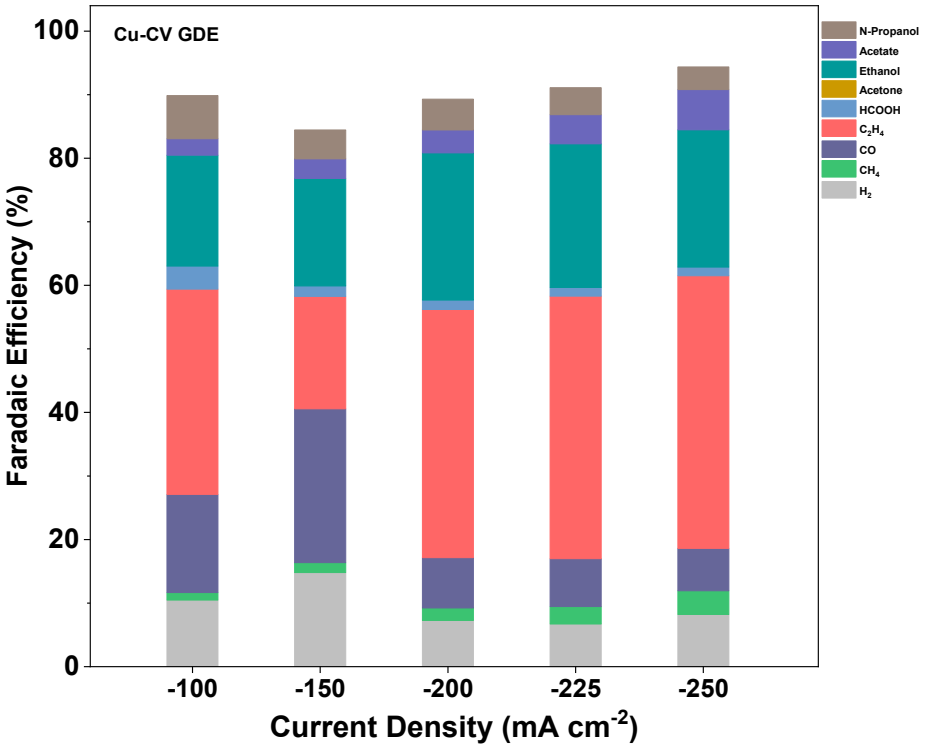

Figure S4. Faradaic efficiency of various products over Cu-CV GDE under the current densities of -100~-250 mA cm^{-2} during the electrocatalytic CO_2 reduction in the flow cell.

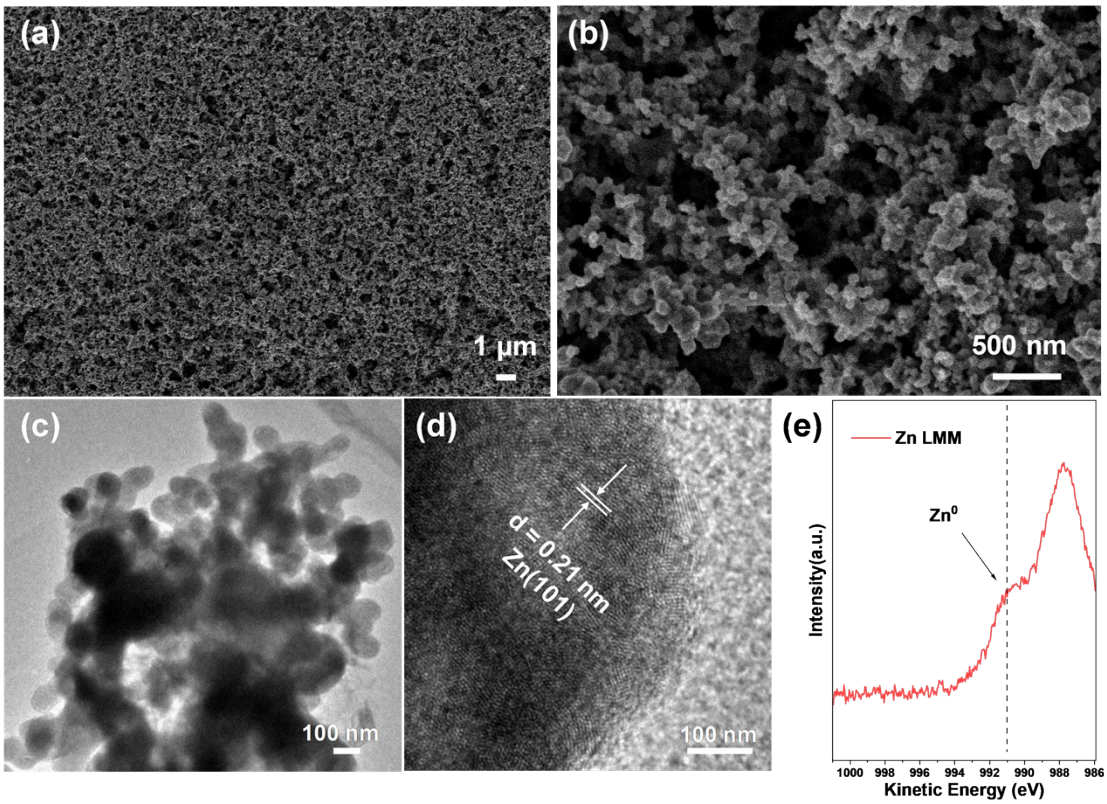

Figure S5. (a) SEM and (b) enlarged SEM image of Zn-GDE electrode; (c) TEM image and (d) HRTEM image of Zn-GDE electrode. (e) XPS spectrum of Zn LMM corresponding to Zn-GDE electrode.

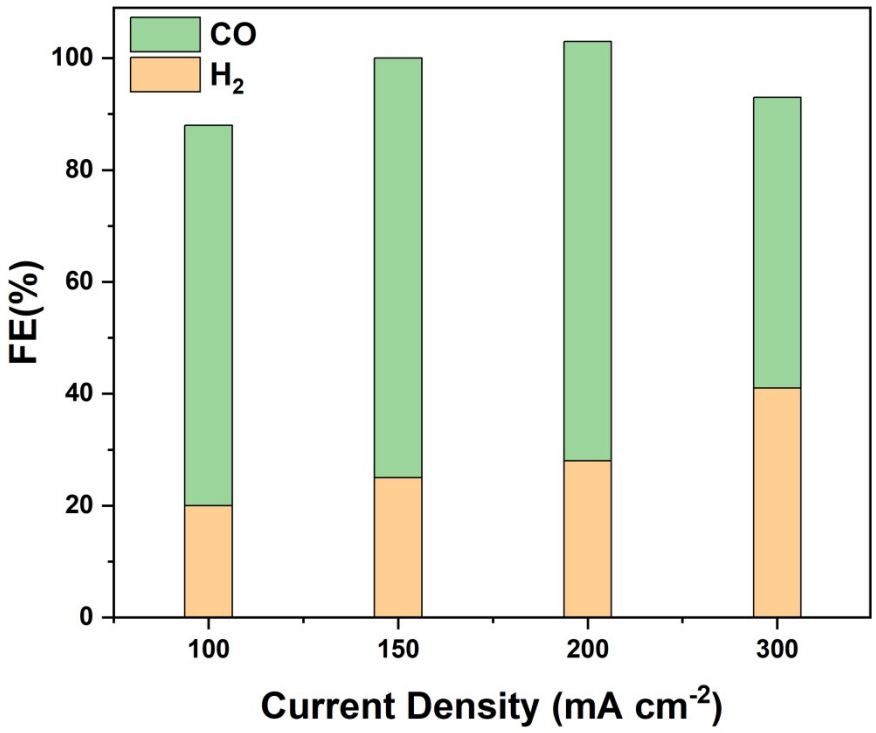

Figure S6. FE of H_2 and CO was the main reduction products at relevant current densities when the electrocatalytic CO_2 reduction performance of the Zn-GDE catalyst was tested in the flow cell.

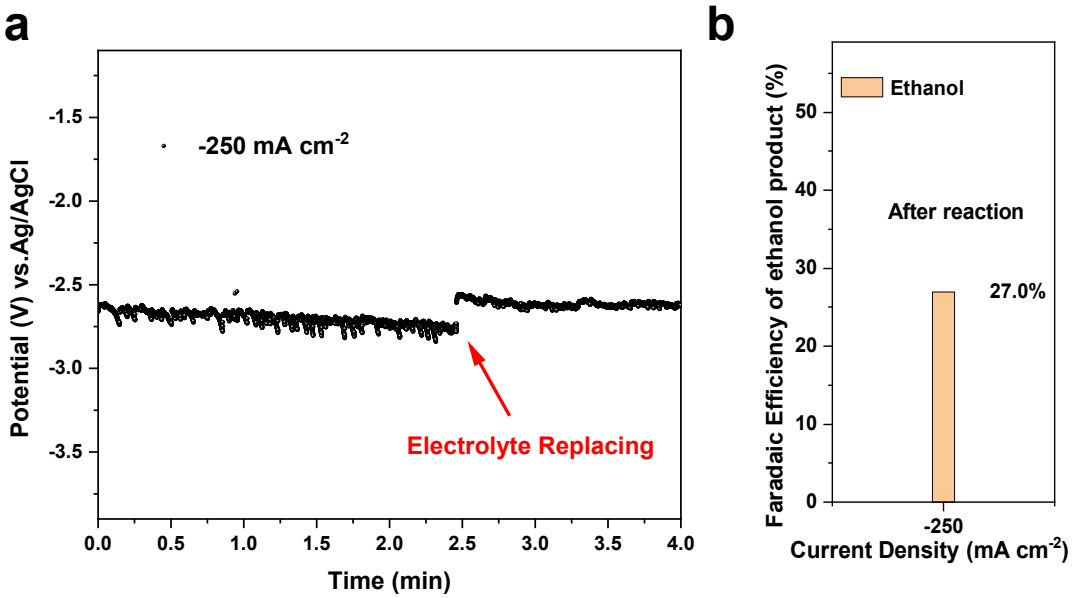

Figure S7. a. The stability of Cu-Zn-CV GDE sample at the current densities of -250 mA cm^{-2}. b. The corresponding Faradaic efficiency of ethanol product after reaction.

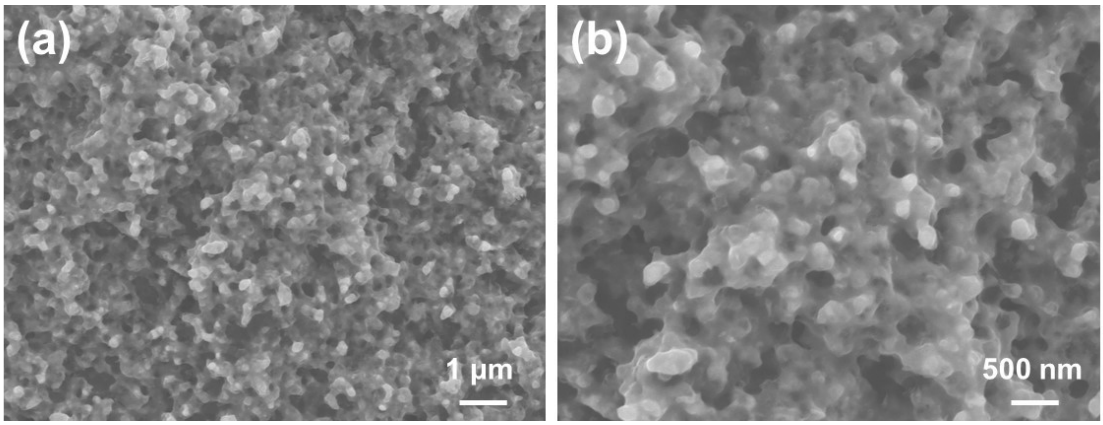

Figure S8. (a) SEM image of Cu-Zn-CV-GDE catalyst and (b) enlarged SEM image after CO_2 reduction reaction.

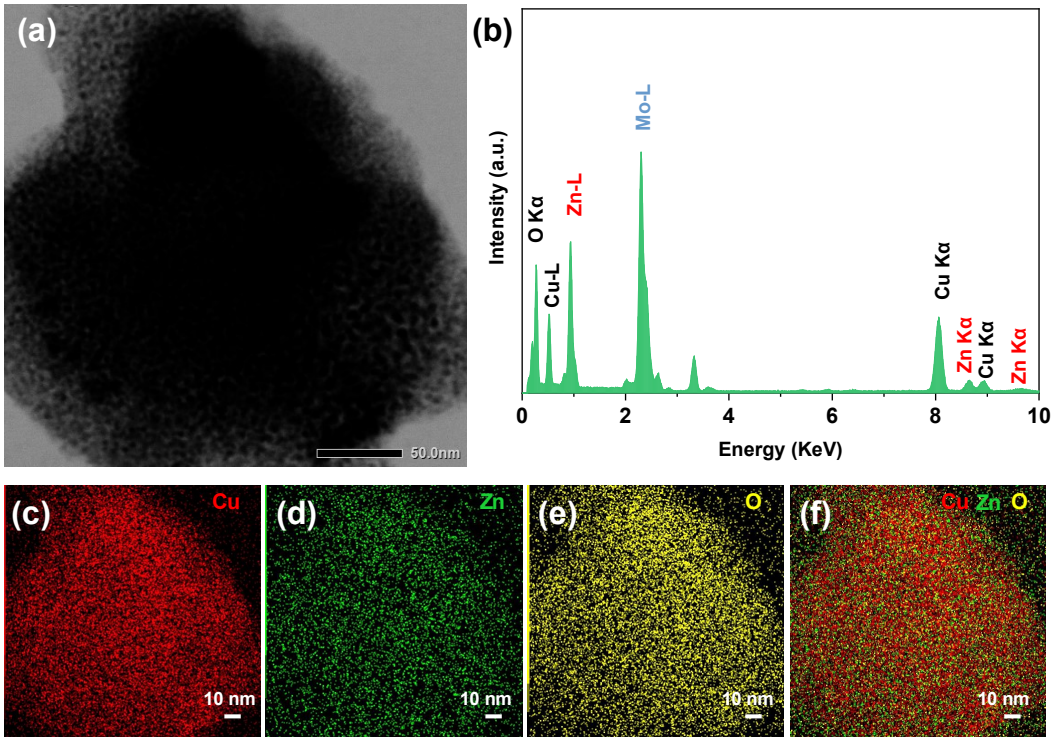

Figure S9. (a) TEM image, (b) EDS image and (c-f) element mapping image of Cu-Zn-CV-GDE catalyst after CO_2 reduction reaction.

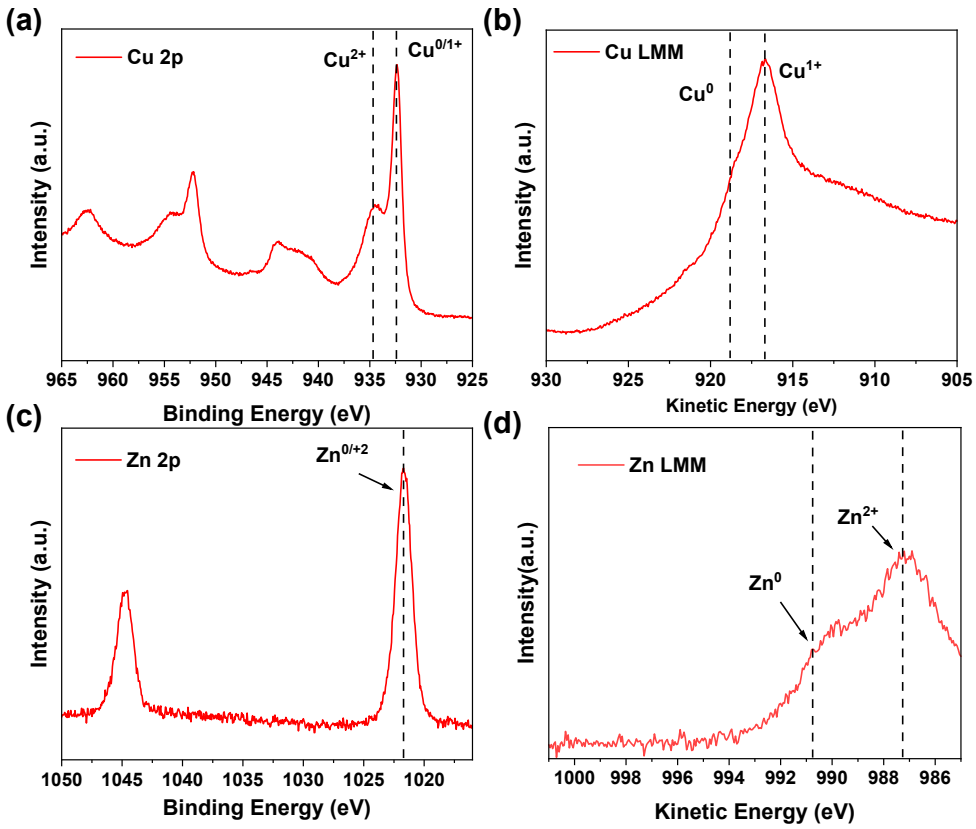

Figure S10. XPS spectrum of Cu-Zn-CV-GDE catalyst after CO_2 reduction reaction, (a) Cu 2p spectrum, (b) Cu LMM energy spectrum, (c) Zn 2p spectrum and (d) Zn LMM energy spectrum.

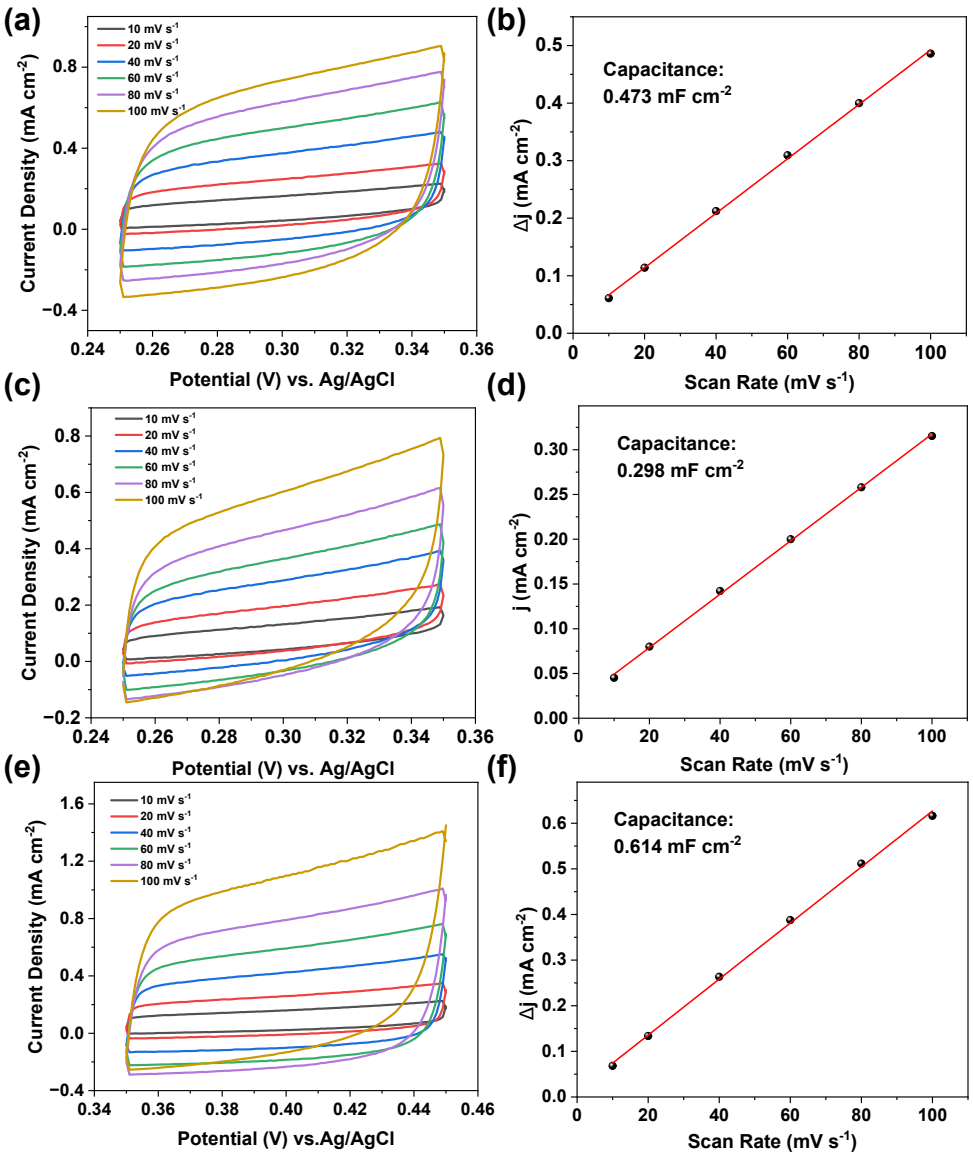

Figure S11. (a) Cu-GDE, (c) Cu-Zn-GDE and (e) Cu-Zn-CV-GDE electrodes in 1.0 M KOH solution at different scan rates (10 mVs^{-1}, 20 mVs^{-1}, 40 mVs^{-1}, 60 mVs^{-1}, 80 mVs^{-1}, 100 mVs^{-1}), (b), (d), (f) and the corresponding electrochemical double layer capacitance.

Table S1 Performance comparison of Cu-based catalysts for CO_2 reduction to ethanol reported in the recent literature.

Catalyst	Electrolyte	$FE_{(Ethanol)}$	Partial Current Density of Ethanol (mA cm^{-2})	Formation rates of ethanol ($\mu mol \cdot m^{-2} \cdot s^{-1}$)	Reference
Cu-500 nm	1.0 M KOH	18.7%	-29.7	--	[1]
CuAg nanowires	1.0 M KOH	25.9%	-80	--	[2]
CuZn-plannar	0.1 M $KHCO_3$	29.1%	-8.2	--	[3]
Ag@C@Cu	1.0 M KOH	31.5%	-126	--	[4]
Cu_9Zn_1	1.0 M KOH	25%	-93	--	[5]
Cu/Cu_2O-Ag-x	1.0 M KOH	19.2%	-58.6	--	[6]
B-Cu-Zn-GDE	1.0 M KOH	31%	-31	--	[7]
Boron-doped Cu	0.1 M $KHCO_3$ 0.1 M KCl	28%	-19	--	[8]
Cu_2S-Cu	1.0 M KOH	25%	-100	--	[9]
CuDAT-wire	1.0 M KOH	27%	-75	--	[10]
CuZn	1.0 M KOH	41.4%	-82.8	--	[11]
Molecule-Cu	1.0 M $KHCO_3$	41%	-124	--	[12]
$CuZn_{20}$/NGN	0.1 M $KHCO_3$	34.2%	-1.35	195	[13]
Cu/Bi-MOFs	0.5 M $KHCO_3$	28.3%	-5.7	17.6	[14]
$dCu_2O/Ag_{2.3\%}$	4.0 M KCl	40.8%	-326.4	1014.9	[15]
Cu-Zn-CV-GDE	1.0 M KOH	29.3%	-73.3	**229**	**This work**

Reference

[1] Ren D, Gao J, Zakeeruddin S M, et al. New Insights into the Interface of Electrochemical Flow Cells for Carbon Dioxide Reduction to Ethylene [J]. The Journal of Physical Chemistry Letters, 2021, 12(31): 7583-7589.

[2] Hoang T T H, Verma S, Ma S, et al. Nanoporous Copper–Silver Alloys by Additive-Controlled Electrodeposition for the Selective Electroreduction of CO_2 to Ethylene and Ethanol [J]. Journal of the American Chemical Society, 2018, 140(17): 5791-5797.

[3] Ren D, Deng Y, Handoko A D, et al. Selective Electrochemical Reduction of Carbon Dioxide to Ethylene and Ethanol on Copper(I) Oxide Catalysts [J]. ACS Catalysis, 2015, 5(5): 2814-2821.

[4] Zhang J, Pham T H M, Ko Y, et al. Tandem effect of Ag@C@Cu catalysts enhances ethanol selectivity for electrochemical CO_2 reduction in flow reactors [J]. Cell Reports Physical Science, 2022, 3(7): 100949.

[5] Baek Y, Song H, Hong D, et al. Electrochemical carbon dioxide reduction on copper–zinc alloys: ethanol and ethylene selectivity analysis [J]. Journal of Materials Chemistry A, 2022, 10(17): 9393-9401.

[6] Su W, Ma L, Cheng Q, et al. Highly dispersive trace silver decorated Cu/Cu2O composites boosting electrochemical CO_2 reduction to ethanol [J]. Journal of CO2 Utilization, 2021, 52: 101698.

[7] Song Y, Junqueira J R C, Sikdar N, et al. B-Cu-Zn Gas Diffusion Electrodes for CO_2 Electroreduction to C_{2+} Products at High Current Densities [J]. Angewandte Chemie International Edition, 2021, 60(16): 9135-9141.

[8] Zhou Y, Che F, Liu M, et al. Dopant-induced electron localization drives CO_2 reduction to C_2 hydrocarbons [J]. Nature Chemistry, 2018, 10(9): 974-980.

[9] Zhuang T-T, Liang Z-Q, Seifitokaldani A, et al. Steering post-C–C coupling selectivity enables high efficiency electroreduction of carbon dioxide to multi-carbon alcohols [J]. Nature Catalysis, 2018, 1(6): 421-428.

[10] Hoang T T H, Ma S, Gold J I, et al. Nanoporous Copper Films by Additive-Controlled Electrodeposition: CO_2 Reduction Catalysis [J]. ACS Catalysis, 2017, 7(5): 3313-3321.

[11] Ren D, Gao J, Pan L, et al. Atomic Layer Deposition of ZnO on CuO Enables Selective and Efficient Electroreduction of Carbon Dioxide to Liquid Fuels [J]. Angewandte Chemie International Edition, 2019, 58(42): 15036-15040.

[12] Li F, Li Y C, Wang Z, et al. Cooperative CO_2-to-ethanol conversion via enriched intermediates at molecule–metal catalyst interfaces [J]. Nature Catalysis, 2020, 3(1): 75-82.

[13] Dongare S, Singh N, Bhunia H. Oxide-derived Cu-Zn nanoparticles supported on N-doped graphene for electrochemical reduction of CO_2 to ethanol [J]. Applied Surface Science, 2021, 556: 149790.

[14] Albo J, Perfecto-Irigaray M, Beobide G, et al. Cu/Bi metal-organic framework-based systems for an enhanced electrochemical transformation of

CO_2 to alcohols [J]. Journal of CO_2 Utilization, 2019, 33: 157-165.
[15]Wang P, Yang H, Tang C, et al. Boosting electrocatalytic CO_2–to–ethanol production via asymmetric C–C coupling [J]. Nature Communications, 2022, 13(1): 3754.